结合型分布带状分段移动热源模型

郑振太[1]， 曹文杰[1]， 许晓航[1]， 单 平[2]， 步贤政[2]
（1. 河北工业大学 材料科学与工程学院，天津 300132；
2. 天津大学 材料科学与工程学院，天津 300072）

摘 要：在数值模拟分析大型焊接结构的焊接残余应力和变形时，可以采用分段移动带状热源模型以便提高计算效率. 为此，首先试验分析了不同焊接速度对焊接温度场带状特性的影响. 并在已建立的结合型分布圆形热源模型的基础上，推导出了结合型分布带状分段移动热源模型的节点热流与加载时间的计算公式. 结果表明，焊接速度大于 4 mm/s时，较长区段的温度场已经具有带状分布特点. 此外，与高斯分布带状分段移动热源模型的节点热流与加载时间的计算公式相比，推导出的公式不但与总的热输入量有关，还与电弧和熔滴的热量分配比有密切的关系.

关键词：大型焊接结构；热源模型；数值模拟
中图分类号：TG402 文献标识码：A 文章编号：0253－360X(2010)07－0095－03


郑振太

0 序 言

随着国内经济建设的蓬勃发展，对大型甚至超大型焊接钢结构的需求越来越多，而且其应用领域也越来越广[1]. 同时，对其制造技术的研究也显得越来越迫切. 由于大型焊接结构造价高、生产周期长等原因，对大尺寸部件及整体结构进行原型尺度的试验研究几乎是不可能的. 而数值模拟研究方法在大型焊接结构的研究方面具有一定的优越性.

由于计算规模庞大以及受到计算机技术发展水平的限制，对于大型焊接结构或部件的数值模拟的研究起步较晚. 自 20世纪末至 21世纪初，国内外的焊接学者均进行了一些实际的大型焊接结构的数值模拟研究[2－8]. 选择某种适宜的热源模型进行数值模拟是十分关键的. 但是，目前仅有采用高斯分布带状分段移动热源模型应用于大型焊接结构的数值模拟.

高斯分布圆形热源模型即通常称谓的高斯热源模型是基于检测 TIG焊接电弧的热流分布而得到的，用于有熔滴过渡的熔化极气体保护焊不一定适合。文中以更适用于有熔滴过渡行为的熔化极气体保护焊的结合型分布焊接热源模型为研究对象，进行了一些研究，以期采用更适合的热源模型进行大型焊接结构的数值模拟研究.

收稿日期：2009－02－16

1 带状热源模型

前苏联的雷卡林院士认为，对于具有一定移动速度的焊接热源，在某个焊缝长度上的作用效果可以近似为带状热源，并可以认为此带状热源同时作用于该长度的焊缝上. 这个思想可以保证在焊接数值模拟中采用相对较大的时间增量步，并进而大大提高计算效率.

在此基础上，清华大学[6]提出了“分段移动带状热源模型”来提高计算效率. 并认为，对于具有一定移动速度的热源，总存在一个焊缝长度可以近似为带状热源，假设此长度为 l，则可将长度为 L的焊缝划分为数段，每段的长度小于等于 l，在每一段内按作用一定时间的带状热源处理，一段段的带状热源按焊接方向顺序施加. 因此，可以用较少的时间增量步描述焊接热源的作用，从而大大减少计算时间. 并且为加载的方便，可将一段带状热源从输入方式上进一步简化为一系列的点热流的同时作用，即分段移动串行热源模型.

从计算效率考虑，l不宜太小. 因此，从工程实用意义而言，是否适合将移动热源近似为带状热源主要决定于焊接速度. 但上述的研究并未给出一个定量的焊接速度值可供参考，为此进行了焊接过程的红外成像试验.

图 1为电弧刚刚熄灭时刻的红外成像的焊接温度场.

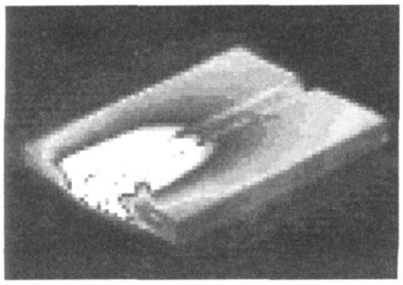

(a) 焊缝长度100 mm，焊接速度1.82 mm/s

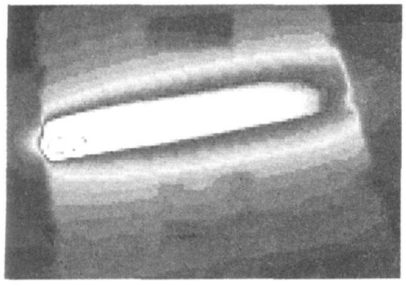

(b) 焊缝长度200 mm，焊接速度4.17 mm/s

图 1 焊接速度对温度场带状特性的影响

Fig. 1 Influence of welding speed on strip characteristics of temperature field

由图 1可见，焊接速度较大时，在较长的区段内温度分布沿焊缝方向成明显的带状；较小时，温度分布仅在很小长度内有带状分布的特征，而且带状特点并不明显．因此，在焊接速度较大时，利用分段移动带状热源模型是比较合理的，而且提高计算效率明显．此外，带状热源模型作用下的数值模拟温度场与速度较大时的温度场试验图像是比较接近的，见图 2．这进一步说明采用分段移动带状热源模型具有一定的合理性．

2 结合型分布带状分段移动热源模型

结合了电弧的高斯分布和熔滴的锥形分布的结合型分布圆形热源模型[9]更适用于热流密度较大的具有熔滴过渡行为的熔化极气体保护焊，例如半自动的短路过渡 CO_2 气体保护焊．欲采用结合型分布带状分段移动热源模型进行数值模拟，首先需要计算节点热流和加载时间，以便编程计算．

2.1 结合型分布移动热源模型的总热输入量

很显然，结合型分布移动热源模型在长度为 l 的焊缝上的总热输入量 Q 为

$$Q = tq = \frac{l}{v}\eta UI \tag{1}$$

式中：t 为焊接时间；q 为焊接有效功率；l 为某段的焊缝长度；v 为焊接速度；η 为焊接热效率；U 为电弧电压；I 为焊接电流．

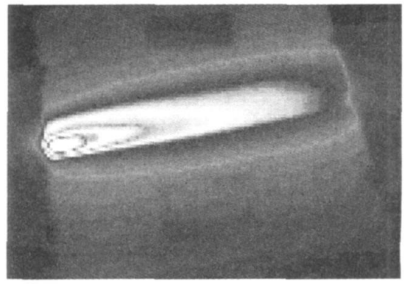

(a) 较快焊接速度红外成像温度场

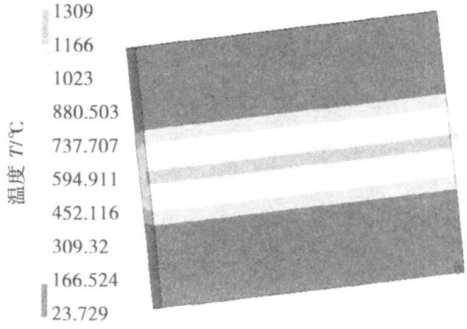

(b) 带状热源模型模拟温度场

图 2 较快速度下的实际焊接温度场与带状热源模型模拟温度场的对比

Fig. 2 Actual welding temperature field in faster welding speed comparing with simulated temperature field of strip-shape heat source model

2.2 结合型分布带状分段移动热源模型总热输入量

结合型分布圆形热源模型热流密度分布为[9]

$$q(r)=\begin{cases}\dfrac{3\eta_d UI}{\pi r_d^2}\left(1-\dfrac{r}{r_d}\right)+\dfrac{3\eta_a UI}{\pi r_a^2}\exp\left(-\dfrac{3r^2}{r_a^2}\right), & r \leqslant r_d \\ \dfrac{3\eta_a UI}{\pi r_a^2}\exp\left(-\dfrac{3r^2}{r_a^2}\right), & r_a \geqslant r > r_d\end{cases} \tag{2}$$

式中：U 为电弧电压；I 为焊接电流；r_a 为电弧热流分布参数；r_d 为熔滴热流分布参数；η_a 为电弧直接输入到焊件中的热效率；η_d 为熔滴输入到焊件中的热效率．

设 $q_d=\dfrac{3\eta_d UI}{\pi r_d^2}$，$q_a=\dfrac{3\eta_a UI}{\pi r_a^2}$，则式 (2)可简化为

$$q(r)=\begin{cases}q_d\left(1-\dfrac{r}{r_d}\right)+q_a\exp\left(-\dfrac{3r^2}{r_a^2}\right), & r \leqslant r_d \\ q_a\exp\left(-\dfrac{3r^2}{r_a^2}\right), & r > r_d\end{cases} \tag{3}$$

式中：q_d 为熔滴热源最大热流密度；q_a 为电弧热源最大热流密度．

如果将长度为 l的焊缝作分段化处理，假设分为 n段，共有 $n+1$个节点，如图 3所示.

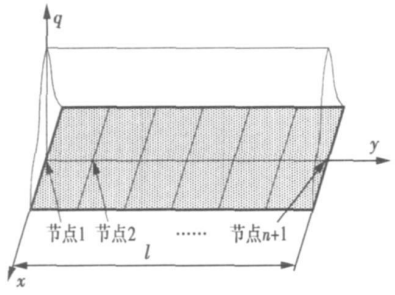

图 3 移动热源分段化处理示意图

Fig. 3 Segmenting of moving heat source

分段化后的在 l长度上的热输入功率 q_2为

$$q_2 = \int_0^l \int_{-\infty}^{\infty} q(x, y)\,dx dy$$

$$= \int_0^l \int_{-\infty}^{r_d} q_a \exp\left(-\frac{3}{r_a^2}x^2\right) dx dy +$$

$$\int_0^l \int_{r_d}^{r_d} \left[q_d\left(1-\frac{x}{r_d}\right) + q_a \exp\left(-\frac{3}{r_a^2}x^2\right)\right] dx dy +$$

$$\int_0^l \int_{r_d}^{\infty} q_a \exp\left(-\frac{3}{r_a^2}x^2\right) dx dy$$

$$= 2\,l q_d r_d + \sqrt{\frac{\pi}{3}}\, l q_a r_a = \left(\frac{6\eta_d}{r_d} + \frac{\sqrt{3\pi}\,\eta_a}{r_a}\right)\frac{UI}{\pi} \tag{4}$$

2.3 节点热流和加载时间

假设分段移动热源在 l长度上的作用时间为 t_1，根据能量守恒原理，未分段的结合型分布移动热源模型在 l长度上的总热输入量与结合型分布分段移动热源模型在 l长度上的总热输入量相等，则有

$$q_2 t_1 = Q_4 \tag{5}$$

将式（1）和式（4）带入式（5）中得到

$$t_1 = \frac{\eta\pi}{\dfrac{6\eta_d}{r_d} + \dfrac{\sqrt{3\pi}\,\eta_a}{r_a}} \cdot \frac{1}{v} \tag{6}$$

由式（6）可见，分段热源加热时间与分段长度 l无关，与焊接速度 v成反比. 高斯热源模型下得到的分段移动热源作用时间的计算公式为[6]

$$t_1' = \sqrt{\frac{\pi}{k}} \cdot \frac{1}{v} = \sqrt{\frac{\pi}{3}}\, r_a \cdot \frac{1}{v} \tag{7}$$

对比式（6）和式（7）可以发现，结合型热源模型的加热时间不仅和热流分布参数及焊接速度有关，还与熔滴和电弧之间的能量分配比有关，显得更加复杂一些. 图 3中每一小段单位时间内输入的热量即热功率为

$$q_3 = \frac{q_2}{n} = \frac{\left(\dfrac{6\eta_d}{r_d} + \dfrac{\sqrt{3\pi}\,\eta_a}{r_a}\right)\dfrac{UI}{\pi}}{n} = \left(\frac{6\eta_d}{r_d} + \frac{\sqrt{3\pi}\,\eta_a}{r_a}\right)\frac{UI}{n\pi} \tag{8}$$

将该热输入功率作用在中部的每个节点上. 两端的节点因均分一小段热输入，故端点处热输入功率为

$$q_4 = \frac{q_3}{2} \tag{9}$$

式（6），式（8）及式（9）的 t_1，q_3及 q_4对结合型热源模型以分段移动串行点热源形式加载进行了完整的具体描述，通过编程便可以用于大型结构的焊接数值模拟中.

3 结　　论

（1）通过对不同焊接速度下的焊件温度场的红外成像试验表明，小于 2 mm/s的焊接速度不宜应用带状分段移动热源模型；而大于 4 mm/s时，较长区段的温度场已经具有典型的带状分布特点，应用该热源模型可以得到较好的数值模拟结果. 而在 2～4 mm/s的焊接速度时宜根据具体焊接条件慎重选用.

（2）经过对结合型分布带状分段移动热源模型的计算系列式的推导可以看出，其关键的热输入参数即加热时间 t_1不仅与焊接速度、热流分布参数相关，还与电弧和熔滴的热量分配比有关.

参考文献：

[1] 林尚扬，关　桥. 我国制造业焊接生产现状与发展战略研究[J]. 金属加工（热加工），2004(5)：10－15.
Lin Shangyang, Guan Qiao. Research on production status and development strategy of welding in China's manufacturing industry[J]. Metal Working (hot working), 2004(5): 10－15.

[2] Brown S B, Song H. Finite element simulation of welding of large structures[J]. Transactions of the ASME, 1992, 114(4): 441－451.

[3] Brown S B, Song H. Implications of three-dimensional numerical simulations of welding of large structures[J]. Welding Journal, 1992, 71(2): 55－62.

[4] 田锡唐，顾福明，高进强，等. 圆柱壳体与法兰对接环形焊缝的焊接变形规律研究[J]. 材料科学与工艺，1996，4(3)：76－80.
Tian Xitang, Gu Fuming, Gao Jinqiang, et al. Research on welding deformations due to circumferential welds at the joint between cylindrical shells and flanges[J]. Material Science and Technology, 1996, 4(3): 76－80.

[下转第 104页]

接系统对两块 H62黄铜进行焊接时，要根据具体情况设置合适的离焦量[6]. 通过改变离焦量来改变激光功率密度的方法是非常方便有效的. 设置一定的离焦量，获得焊接所需合理的激光功率密度，不仅便于焊接而且容易获得美观牢固的焊缝[7]；避免由于激光功率密度过大而使母材汽化，形成火花，造成飞溅等不良后果；能够加宽焊缝. 一般地，若希望熔深较大，则采用负离焦的方式；若对熔深要求不高，则采用正离焦的方式. 在用 HWIW—300A型激光焊接系统对厚度为 2.5 mm的两铜板进行对接焊时，采用负离焦 2 mm的方式进行焊接能获得较好的焊接效果.

3 结 论

(1)用 HWIW—300A型能量负反馈脉冲激光焊接系统能对厚度为 2.5 mm的两块 H62黄铜成功地进行焊接. 焊接过程中由于锌的部分蒸发及在蒸发时带走了部分铜，再加上待焊接的两块黄铜间不可避免地会有缝隙(即材料缺少)等因素，所以焊接后会形成凹陷的焊缝.

(2)在用脉冲激光焊接时要合理设置工艺参数. 激光功率及单脉冲能量直接决定焊接的成功与否，调节离焦量可以方便地调节激光束的功率密度，激光束的单脉冲能量太大或太小都不能得到满意的焊接效果. 在对两块厚度为 x(mm)的 H62黄铜进行对接焊时，单脉冲激光能量一般取 10·x(J/mm)；通过试验验证和理论分析得知，快速上升、缓慢下降的激光波形有利于对 H62黄铜进行焊接.

(3)在用脉冲激光进行焊接时，相邻焊点间应有合适的重叠量. 通常使激光光斑直径 d脉冲频率及焊接速度 v间满足 f·d=(1.2~1.4)·v关系.

参考文献：

[1] 王运炎. 机械工程材料[M]. 北京：机械工业出版社，1993

[2] 皮友东，董 鹏，杨武雄，等. 黄铜—低碳钢异种金属激光深熔钎焊[J]. 中国激光，2007，34(11)：1562—1566
Pi Youdong, Dong Peng, Yang Wuxiong, et al. Laser penetration brazing of brass and low carbon steel[J]. Chinese Journal of Lasers, 2007, 34(11): 1562—1566

[3] 王 迪，杨永强，师文庆. H62黄铜激光焊接工艺与组织特征研究[J]. 应用激光，2009，29(3)：203—206
Wang Di, Yang Yongqiang, Shi Wenqing. Investigation on laser welding process and structure characteristics of H62 copper[J]. Applied Laser, 2009, 29(3): 203—206

[4] 季 杰，马学智. 铜及铜合金的焊接[J]. 焊接技术，1999，4(2)：13—15
Ji Jie, Ma Xuezhi. Welding of copper and copper alloy[J]. Welding Technology, 1999, 4(2): 13—15

[5] 王振家，欧向军，陈武柱，等. H62黄铜激光焊接性的研究[J]. 清华大学学报，1997，37(8)：40—43
Wang Zhenjia, Ou Xiangjun, Chen Wuzhu, et al. Study on weldability of H62 brass by laser welding[J]. Journal of Tsinghua University, 1997, 37(8): 40—43

[6] 朱传运，王振家. 焦点位置的确定和 H62黄铜激光焊接性的研究[J]. 热加工工艺，2008，37(4)：58—60
Zhu Chuanyun, Wang Zhenjia. Selecting focus position and laser weldability of H62 brass[J]. Hot Working Technology, 2008, 37(4): 58—60.

[7] 张国顺. 现代激光制造技术[M]. 北京：化学工业出版社，2005.

作者简介：师文庆，男，1971年出生，博士研究生，讲师. 主要从事物理电子及激光技术方面的科研和教学工作. 发表论文 20余篇.
Email: swqaff@163.com

[上接第 97页]

[5] 田锡唐，顾福明，高进强，等. 圆柱壳体上环形焊缝焊接变形的数值分析[J]. 航空材料学报，1996，16(2)：50—56
Tian Xitang, Gu Fuming, Gao Jinqiang, et al. Numerical analysis for welding deformations due to circumferential welds in cylindrical shells[J]. Journal of Aeronautical Materials, 1996, 16(2): 50—56

[6] 蔡志鹏. 大型结构焊接变形数值模拟的研究与应用[D]. 北京：清华大学，2001.

[7] Nishikawa Hiroyasu, Serizawa Hisashi, Murakawa Hidekazu. Actual application of large-scaled FEM for analysis of mechanical problems in welding[J]. Quarterly Journal of JWS, 2006, 24(2): 168—173.

[8] 郑振太. 大型厚壁结构焊接过程的数值模拟研究与应用[D]. 天津：天津大学，2007.

[9] Zheng Zhentai, Shan Ping, Hu Shengsun, et al. Numerical simulation of gas metal arc welding temperature field[J]. China Welding, 2006, 15(4): 55—58.

作者简介：郑振太，男，1966年出生，博士，教授. 主要研究方向为焊接数值模拟. 已发表论文 32篇.
Email: zzt@hebut.edu.cn

ing systems in welding robot the camera model in Open Source Computer Vision Library(OpenCV) was discussed a profound investigation of the camera calibration process and geometric model was performed Specially the radial distortion and tangential distortion had been taken into account Then the Bouguet corner point s extraction algorithm was applied and a camera calibration algorithm based on OpenCV was implemented The results show that the algorithm gives full play of the functions in OpenCV library and extracts the checkboard corners successfully both the precision and computational efficiency are improved Therefore it can satisfy the requirements of real-time performance in camera calibration of vision navigation system.

Key words: seam tracking; vision guidance; camera calibration; OpenCV; planar template

Finite element analysis and nanoindentation-based experiment of residual stress of SS304/BNi-2/SS304 stainless steel brazed joints LI Guo1, GONG Jianming1, CHEN Hu2 (1. School of Mechanical and Power Engineering, Nanjing University of Technology, Nanjing 210009, China; 2. Technical Development Department, Ningbo Special Equipment Inspection and Test Center, Ningbo 315020, Zhejiang, China). p79—82, 86

Abstract: The numerical analysis was implemented on the residual stress of the SS304/BNi-2/SS304 T shape brazed joint by both finite element method (FEM) employing ABAQUS sequentially coupling code and Nanoindentation technology. The results show that the residual stress of the brazed joint produced due to the mechanical property mismatch of the base metal SS304 and the filler BNi-2. The residual stress which can induce the crack initiation and is maximum at the fillet and decreases gradually along the mid-seaming. The other zone is uniformity. So the fillet becomes the weakest area. The Nanoindentation test adopts the Suresh model and the experimental results are corresponded with the FEM and also prove the efficient and reliability of FEM.

Key words: brazing; nanoindentation; residual stress; finite element; T shape joint

Influence factors of fatigue strength assessment for welded joints by hot spot stress approach PENG Fan, YAO Yunjian, GU Yongjun (College of Mechanical and Vehicle Engineering, Hunan University, Changsha 410082, China). p83—86

Abstract: The fatigue notch factors of welded joints are expressed in terms of hot spot stress serving as controlling stress and obtained on the basis of Taylor's Critical Distance Theory corresponding to three approaches to determine hot spot stress. The effects of joint types, weld sizes, main plate thickness and the methods to determine the hot spot stresses on the fatigue assessment of welded joints are examined with the analysis of fatigue notch factors. The results show that the influence of weld size and the web plate thickness on the scatter of fatigue notch factors is small in contrary to the obvious effect of the main plate thickness, and the latter is predicted for welded joints of fillet welds and butt welds respectively by means of fatigue notch factors and is found to be in good agreement with existing empirical relation. Also it is indicated that the two types of extrapolation method to obtain hot spot stresses are valid in reducing the diversity of fatigue data and the dependence of fatigue data on the types of joints and loading conditions.

Key words: welded joints; fatigue strength; hot spot stress; critic distances theory; fatigue notch factor

Effect of magnetic field on twin-wire indirect arc shape ZHANG Shunshan, WU Dongting, ZOU Zengda, QU Shiyao (Key Laboratory for Liquid-Solid Structural Evolution & Processing of Materials, Ministry of Education, Shandong University, Jinan 250061, China). p87—90

Abstract: The effect of internal magnetic field and external magnetic field on twin-wire indirect arc shape was studied in this paper. The variation of internal magnetic field was obtained by changing the angle of wires. The external magnetic field was applied by excitation coil. The magnetic induction intensity was measured by Teslameter, and the indirect arc shapes were captured by high-speed camera system. The experimental results showed that the magnetic intensity difference between the internal and external region of arc increased by decreasing of the included angle and increasing of applied transverse external magnetic intensity. As a result, which increased the extrapolation effect of electromagnetic force and the arc became long and concentrated. Applied longitudinal external magnetic field would deflect the indirect arc in the vertical plane of the twin wires, and the deflection degree increased with increasing of applied longitudinal external magnetic intensity.

Key words: twin wires welding; indirect arc; arc shape

Mathematical model for NC cutting saddle type of welding groove with edge CHEN Yongliu, BAI Xue (School of Mechanical & Power Engineering, Harbin University of Science and Technology, Harbin 150080, China). p91—94

Abstract: This paper is based on the establisment of the mathematics model for saddle type welding groove with the edge, given the geometric definition of the edge curves, the influence of the different cutting tracks to the principle error Δb of the height of the edge was discussed. The length change Δm of groove generatrix has an effect on the distance a between cutting torch and workpiece, the eliminate method that the existence of Δm which causes the distance between cutting torch and workpiece changes Δa is introduced. The establisment of the mathematical model for saddle type welding groove with the edge by the welding groove geometric model to calculate the Δm and set the method of Δm and cutting intersection angle θ curves is descriked. It concluse that using the edge curves as the cutting tracks can eliminate the change of Δa caused by the Δm and improve the cutting quality and accuracy.

Key words: welding; NC cutting; intersecting line; welding groove; saddle type; mathematics model

Segment-moving heat source model with strip-shape and combined distribution of heat flux ZHENG Zhentai,

CAO Wenjie, XU Xiaohang, SHAN Ping, BU Xianzheng (1. School of Materials Science and Engineering, Hebei University of Technology, Tianjin 300132, China; 2. School of Materials Science and Engineering, Tianjin University, Tianjin 300072, China). p 95—97, 104

Abstract: Segment-moving heat source model of strip-shape is high computational efficiency in the numerical simulation of the welding residual stress and distortion of large welded structures. To improve the computational efficiency, the influence of the different welding speed on the strip characteristics of welding temperature field is analyzed by experiments. And expressions of node heat flow and loading time in the segment-moving heat source model with the strip-shape and combined distribution of heat flux are derived based on the established circular heat source model of the combined distribution of heat flux. The results show that the longer section of the temperature field has already the strip shape as the welding speed is more than 4 mm/s. In addition, comparing with the expressions of node flow and loading time of segment-moving heat source model with the strip-shape and Gaussian distribution of heat flux, the derived expressions relate to not only the heat input sum but also the heat splitting ratio of arc and droplet.

Key words: large welded structure; heat source model; numerical simulation

Influence of active flux to butt weld and T type penetration weld of TA15 titanium alloy TIG weld DU Yuxiao, WANG Dapeng, GUO Delun, LI Xiaohong, ZHANG Lianfeng, NI Jiaqiang (1. BAMTRI, Beijing 100024, China; 2. Shenyang SAC, Shenyang 110034, China). p 98—100, 108

Abstract: Penetration welding is an important welding type in titanium thin sheet structures. Based on the analysis about welding parameter, weld shape, porosity, weld microstructure, tensile property, bending property and gas amount, the influence of the A-TIG technique on penetration welding joint of the TA15 titanium alloy was investigated, also the contrast between penetration weld and butt weld was investigated. The results show that the A-TIG technique could make the similar influence on such respects as welding parameter, weld shape, porosity, weld microstructure, and gas amount to the both penetration weld and butt weld, also the similar influences of A-TIG on the tensile property, bending property to the penetration welding and the butt weld.

Key word: active flux; penetration weld; titanium alloy

Study on pulse laser welding of H62 brass SHI Wenqing, YANG Yongqiang, WANG Di, HUANG Dongling (1. School of Mechanical & Automotive Engineering, South China University of Technology, Guangzhou 510640, China; 2. College of Science, Guangdong Ocean University, Zhanjiang 524088, Guangdong, China). p 101—104

Abstract: In order to conduct laser welding of H62 brass which has high reflectivity for laser beam with wave length of 1.06 μm, such parameters as pulse laser peak power, laser frequency, single pulse energy, pulse width, pulse waveform, welding speed and defocusing amount etc are reasonably set up through theoretical analysis and experimental verify. H62 brass can be welded by pulse laser successfully. The results show that the pulse laser welding system of HWLW-300A which possess single pulse energy of about 10^{x} (J/mm), the pulse waveforms of sudden rise and slow fall, the defocusing amount of -2 mm and the relationship among laser beam diameter d, pulse laser frequency f and welding speed v meet the $f = (1.2 \sim 1.4)^{x} v$ can successfully weld H62 brass with thickness of x mm.

Key words: laser technology; laser welding; H62 brass; influencing factors

Analysis on weld quality and stability by triple-electrode high speed CO_2 welding MA Xiaoli, HUA Xueming, LIN Hang, WU Yixiong (1. Shanghai Key Laboratory of Materials Laser Processing and Modification, Shanghai Jiaotong University, Shanghai 200240, China). p 105—108

Abstract: The effect of welding currents and welding speed on bead appearance and shape of triple-electrode high speed CO_2 fillet welding on double sides was investigated. It was found that the current of leading electrode should be the highest and current difference between leading electrode and middle electrode had better be 100 A or above to obtain good weld quality. The current difference between middle electrode and trailing electrode don't play an obvious role in weld quality and the electrode offset should be at flat plate. Welding process stability was analyzed through current and voltage acquisition signals characteristic parameters on LabVIEW and high speed photograph. It indicated that the voltage fluctuation increased with the increment of welding speed, the fluctuation by 400/300/300 A combination is the lowest at the same welding speed, and the inter-wire distance should be increase to decrease the arc interference.

Key words: triple-electrode high speed CO_2 welding; welding currents; welding speed; weld stability; arc interference

Heat conduction models and analysis for HAZ of plate welding ZHANG Fangfang, FANG Zhaohong (School of Thermal Energy Engineering, Shandong Jianzhu University, Jinan 250101, China). p 109—112

Abstract: Three thermal conduction models, i.e. the transient planar heat source model, the initial temperature of molten pool model and the moving heat source model, are presented to describe the temperature development in the vicinity of a long welding line in a large flat plate. Analytical solutions are given for these models. Based on these solutions, the relation between the temperature and the width of the heat affected zone is derived with explicit functions. Furthermore, the criterion was proposed to indentify for the impact of the heat dissipation from the plate surface on the conduction process.

Key words: welding; HAZ; heat conduction model